

REASONS EXPERIMENTS CAN BE PERFORMED AT A
pp MACHINE AT $L = 10^{33} \text{ cm}^{-2} \text{ sec}^{-1}$

H.A. Gordon, T. Ludlam, E. Platner, and M.J. Tannenbaum
Brookhaven National Laboratory, Upton, New York 11973

Examples of experiments that cope with high rate environments are given. Then the factors which lead to the conclusion that experiments can be performed at $L = 10^{33} \text{ cm}^{-2} \text{ sec}^{-1}$ in pp collisions at $\sqrt{s} = 800 \text{ GeV}$ are discussed.

I. Performance of Existing Hardware

A. Wire Chambers

1. MPS-II. This year the MPS-II drift chamber system has gone into operation in a most impressive way.¹ The chambers have a maximum drift distance of 3 mm which corresponds to maximum drift time of 55 nsec, and an anode to cathode spacing of 6 mm. They run at a gas gain of 10^5 . An experiment to study the reaction $\pi^- p \rightarrow \phi \phi n$ has collected ≈ 1000 events, the largest statistics for this reaction ever studied. In the course of this experiment, beams of 3×10^6 routinely went through the center of the chambers. At a rate of 10^5 charged particles/cm²/sec or 3×10^4 charged particles/mm of anode wire, a 5% degradation of the efficiency of the chambers was measured due to space charge. A single anode wire could count $\approx 10^6$ charged particles before any loss set in.

2. Axial Field Spectrometer at the CERN ISR (R807).² The drift chamber has the so-called bicycle wheel geometry. The anode to anode spacing is 1.4 cm at the inner radius of 20 cm and 5.6 cm at the outer radius. This corresponds to a maximum drift time of ≈ 140 nsec at the inner radius and ≈ 560 nsec at the outer radius. In 1981 for a short time the drift chamber, which covers $\Delta y = 2$ about 90° , recorded events at $1.2 \times 10^{32} \text{ cm}^{-2} \text{ sec}^{-1}$. The tracks in these events were found by the standard program with only a modest increase in computer time and showed similar characteristics to events taken at lower luminosity. There has been some reluctance to run the drift chamber routinely at this high luminosity due to concern for the chamber lifetime. Silicon deposits have been found on anode wires of test chambers with similar construction and the same gas used after 10^{16} avalanche electrons or 5×10^{10} charged tracks/cm² for an avalanche gain of 1.5×10^4 . At this point a 5% reduction in gain was observed. This would predict a 15% reduction in gain in the actual drift chambers after 2 ISR years of running at $10^{31} \text{ cm}^{-2} \text{ sec}^{-1}$. We do not know if such a reduction in gain occurred in the actual drift chambers in the experiment. The cause of these deposits is not known for certain; however, it may well be due to the gas. If this turns out to be true a small chamber in series with the gas delivery system may be used to take out the silicon with no deterioration of the main drift chambers. Even though these chambers were not designed for high luminosity, they work at $\approx 10^{32}$ and probably the lifetime question is related to the gas system and therefore inconsequential.

3. R-108 Experience with Iron Low β at ISR. This detector has been in operation at the ISR since 1977 routinely running with the original iron low β quadrupoles at luminosities of $5 \times 10^{31} \text{ cm}^{-2} \text{ sec}^{-1}$.³ The drift chambers have a sense-field spacing of 13 mm at a radius of 20 cm from the beam and 22 mm at 64 cm

radius. The anode to cathode distance is 3 mm in all cases and the chambers are located in a magnetic field of 1.4 Telsa. Each sense wire has a delay line to measure the third dimension. Each sense wire and delay line covers a rapidity range of 2.8 units and 1/48 of the full azimuth at the inner radius, and 1.8 units of rapidity and 1/90 of the full azimuth at the outer radius. The maximum delay times from t_0 for a track (including drift time and delay line) was 440 nsec at the inner radius and 800 nsec at the outer radius. The total number of sense wires in the detector was only 580. In documents to the ISRC in 1977-1978⁽⁴⁾ relevant to the superconducting low β , this group said that "We believe that the present system will work well up to luminosities around $10^{32} \text{ cm}^{-2} \text{ sec}^{-1}$ and "By reducing wire spacing, the chambers will work very well at luminosities of $2-3 \times 10^{32} \text{ cm}^{-2} \text{ sec}^{-1}$."⁴

4. Fermilab 288/494/605 Experience⁽⁵⁾. These experiments evolved from experience with high rates in a fixed target environment. Beam fluxes of up to 3×10^{10} per spill for bare target running up to 7×10^{11} per spill with a hadron filter were incident on a 30% interaction length target. The rate on the PWC's at the front of the apparatus was $\approx 2-3 \times 10^7$ with 2 mm wire spacing.

B. Calorimeters

1. ISR Experience. The four liquid argon calorimeters in experiment R806 at the CERN-ISR each routinely collected data at $1-3 \times 10^{31} \text{ cm}^{-2} \text{ sec}^{-1}$. They each covered a solid angle of ≈ 1 steradian. The shaping time was $\approx 1 \mu\text{sec}$. To reject background from pile up of close events in time, a zero crossing discriminator was used as in low energy physics.

R807 is just bringing into operation the uranium-scintillator electromagnetic and hadron calorimeter. It now covers the full azimuth and $\pm 40^\circ$ around 90° . The calorimeter has been tested at the top ISR luminosity of $10^{32} \text{ cm}^{-2} \text{ sec}^{-1}$ with a gate width of 120 nsec with no obvious change from the performances at lower luminosities. Double events at this luminosity can be observed in the timing signals of the highly segmented beam-beam counters or in the timing of the calorimeter signals themselves.

The lead-glass shower counters of R108 at the CERN ISR routinely collected data at $7 \times 10^{31} \text{ cm}^{-2} \text{ sec}^{-1}$. During filling of the ISR the lead-glass blocks had to be retracted to prevent radiation damage.

II. Prospects for Operating at $10^{33} \text{ cm}^{-2} \text{ sec}^{-1}$ at $\sqrt{s} = 800 \text{ GeV}$

The recent data from the SPS pp collider gives an estimate of what to expect for pp collisions at $\sqrt{s} = 800 \text{ GeV}$. At $\sqrt{s} = 540 \text{ GeV}$, $\sigma_{\text{Total}} = 66 \pm 7 \text{ mb}$. The elastic cross section is $\approx 10 \text{ mb}$; therefore, we will assume that the inelastic cross section is 50 mb. At $L = 10^{33} \text{ cm}^{-2} \text{ sec}^{-1}$ this corresponds to one event every 20 nsec. UA1 finds $dn(\text{charged})/dy = 3.6 \pm 0.3$ for all events. We assume this is still the value at $\sqrt{s} = 800 \text{ GeV}$ and that the neutral multiplicity is $dn_0/dy = 1.8$.

A. Drift Chamber

Assume a maximum drift spacing of 2 mm and a 4 mm anode to anode spacing in a cylindrically symmetric drift chamber. If the inner radius starts at 20 cm from the intersection diamond, there could be $2\pi \times 20 \text{ cm} / 0.4 \text{ cm} = 314$ wires in circumference. Assume the drift chamber were split at 90° so that a single wire would extend for 1.5 units of rapidity on either side of 90° . The rate on that wire (the worst case for the drift chamber) would be 50×10^6 interactions/sec \times 3.6 charged particles per unit of $y \times (1.5 \text{ units of } y) / 314 \text{ wires} \approx 10^6$ particles/wire/sec. This rate is acceptable by a system such as the MPS-II system. Clearly the space charge problem could be reduced in the MPS-II system by reducing the cathode to anode distance and by reducing the gas gain. However, even holding those parameters as they exist for the MPS-II results in a manageable rate. Of course a scintillator hodoscope will be required especially on the outer radius of the drift chamber to enable the elimination of tracks from out of time events.

Two approaches may be considered to handle even higher luminosities. The MIT plan of keeping the drift chamber for muons outside of a calorimeter which absorbs most of the charged particles probably allows the use of $L = 10^{34} \text{ cm}^{-2} \text{ sec}^{-1}$.⁶ Multiple scattering in the calorimeter/absorber does not significantly reduce the mass resolution since the muons are nearly back-to-back. Alternatively, a strong magnetic field can be used to trap particles of low momentum. For example, a field of 5T at a radius of 1 m will reduce the number of charged particles outside this radius by a factor of ≈ 10 .

B. Calorimeters

There are two separate considerations of the effect of using calorimeters at high luminosities: (1) how the pileup of many events may simulate a false trigger and (2) how the pileup of extra events affects the analysis of real triggers. To quantitatively assess these, we used ISAJET⁷ to generate minimum bias events. We added sequential events together to correspond to $\bar{n} = 1, 5$ and 10 events but distributed with a Poisson distribution. $\bar{n} = 1$ represents the problem at the trigger level if the trigger is sensitive to a time resolution of 10-20 nsec. $\bar{n} = 5$ represents a typical gate for a scintillator calorimeter or lead glass shower counter of 100 nsec. $\bar{n} = 10$ represents a typical gate for a PWC calorimeter or a liquid argon calorimeter. The results are summarized in Table I.

We feel it is essential for any calorimeter to be segmented into towers in a high rate environment. Lead glass can easily be segmented into towers. The CDF design at Fermilab has towers for both the electromagnetic and hadronic calorimeters both in the scintillator and PWC sections of the calorimeters. Even liquid argon calorimeters can be segmented as demonstrated by the TASSO detector.⁸ For this study, the calorimeter consisted of a cylinder divided uniformly in rapidity (y) and azimuth (ϕ) into 40×40 cells covering $-2 < y < 2$ and $0 < \phi < 2\pi$. There is no distinction made in this study between electromagnetic and hadronic energy. In Fig. 1 is shown the $\Sigma |P_T|$ for the full calorimeter $\Delta y = 4$, $\Delta\phi = 2\pi$. Clearly, this type of sum is not too useful.

One should make a decision about what the physics focus is before a more detailed consideration of the pile up. For W^\pm and Z^0 physics triggering on 1 or 2 electrons a large signal is required in 1 or 2 small areas (towers). Then the average P_T/tower listed in

Table I is relevant. Of course the fluctuations in the tail of the distribution, seen in Fig. 2, are the most serious concern. Fig. 2 shows the rate of $\bar{n} = 10$ events piled up (a worst case) in the section of the calorimeter ($\Delta y = 0.1$, $\Delta\phi = 9^\circ$) which has the largest P_T . The highest P_T bins are made up of a small number of particles rather than the overlap of many small P_T contributions. Also shown is the expected π^0 single particle spectra.⁶ Clearly, above $\approx 5 \text{ GeV}/c$ the real π^0 's dominate the false triggers. In using the high luminosity, looking for π^0 's, γ , e^\pm , W 's, Z^0 , etc., one would obviously have a threshold greater than 20 GeV (at least) to reduce the trigger rate and at that value the false triggers are negligible.

For the study of events involving hadron jets a larger region of the calorimeter will be required, eg., $\Delta y = 1$, $\Delta\phi = \pi/2$. Fig. 3 shows the rate of false triggers for $\bar{n} = 10$ events. Again, this represents a worst case since the trigger should have a time constant of $\approx 10\text{-}20$ nsec even for slow charge collection times. Also shown is the ISAJET prediction for the inclusive single jet cross section.⁷ Beyond about 10 GeV the true jets dominate the false pile up triggers.

To assess the effect of the pile up on a real jet trigger, consider the $\langle \Sigma |P_T| \rangle$ in a fixed location of size $\Delta y = 1$, $\Delta\phi = \pi/2$ as shown in Fig. 4. The mean is $\approx 3.05 \text{ GeV}/c$ in this size interval. However, if a tower is required to have greater than 1 GeV before it contributes to the sum, the $\langle \Sigma |P_T| \rangle = 0.35 \text{ GeV}/c$, and the distribution dramatically narrows as is also shown in Fig. 4. This means that if a real jet were in such a region of the calorimeter and the 1 GeV/c P_T threshold were used, the pile up of even 10 events would only contribute an average of 0.35 GeV/c to the true jet. Since this distribution falls so much more steeply than the true jet production, the tail of the distribution does not make a significant contribution.

Conclusion

On the basis of experience with existing detectors we conclude that drift chambers and calorimeters can be designed to operate in the rate environment of $L = 10^{33} \text{ cm}^{-2} \text{ sec}^{-1}$. Furthermore, a detailed Monte Carlo study shows that the presence of pile up events in calorimeter data at this luminosity need not produce unacceptable backgrounds either at the trigger level or in the analysis of triggered events.

This research was supported by the U.S. Department of Energy under contract DE-AC02-76-CH00016.

References

1. A. Etkin et al., IEEE Trans. Nucl. Sci. NS-26, No. 2, 54 (1979).
2. H. Gordon et al., The Axial Field Spectrometer at the CERN ISR CERN-EP/81-34 (1981).
3. L. Camilleri et al., NIM 156, 275 (1978).
4. CCOR Collaboration, CERN ISRC/78-3 (1978).
5. R. McCarthy, private communication.
6. G. Bunce et al., W, Z^0 Production at a PP Collider, these proceedings.
7. F.E. Paige and S.D. Protopopescu, ISAJET: A Monte Carlo Event Generator for ISABELLE, BNL 29777.
8. V. Kadansky et al., Physics Scripta 23, 680 (1981).

Table I. Effect of Pileup in Calorimeter from \bar{n} Minimum Bias Events*

	$\bar{n} = 1$	$\bar{n} = 5$	$\bar{n} = 10$
<# of Towers> Hit (out of 1600)	27 (19)	132 (67)	250 (86)
< ΣP_T > $ y < 2$	8.0 (5.7)	40 (22)	79 (30) GeV
Average P_T /tower	5	26	50 MeV
<Largest P_T in> a Tower	0.86 (0.39)	1.33 (0.45)	1.59 (0.41) GeV
< ΣP_T > $\Delta y = 1$ $\Delta\phi = \pi/2$	0.31 (0.45)	1.54 (1.24)	3.05 (1.7) GeV
< ΣP_T > $\Delta y = 1$ $\Delta\phi = \pi/2$ Only if $P_T^i > 1$ GeV	0.02 (0.19)	0.13 (0.47)	0.35 (0.7) GeV
<Largest P_T > in any $\left. \begin{array}{l} \Delta y = 1 \\ \Delta\phi = \pi/2 \\ P_T > 1 \end{array} \right\}$ interval	0.86 (0.39)	1.40 (0.91)	2.22 (1.0) GeV

*The numbers in parentheses give the second moments (rms widths) of the indicated distributions.

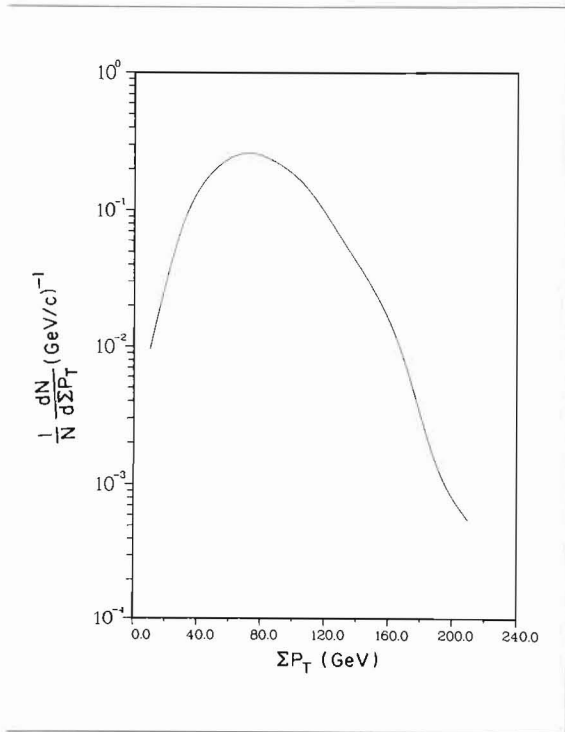


Figure 1. Sum of $|P_T|$ for $|y| < 2$. $\bar{n} = 10$ events.

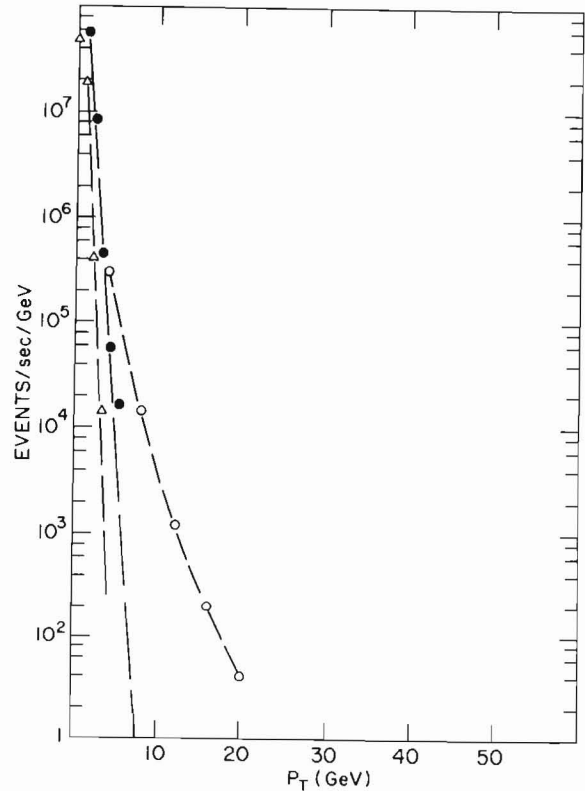


Figure 2. Rate of false triggers for the tower ($\Delta y = 0.1$, $\Delta\phi = 9^\circ$) with the largest P_T vs. P_T from $\bar{n} = 10$ minimum bias events in pp collisions at $\sqrt{s} = 800$ GeV and $L = 10^{33} \text{ cm}^{-2} \text{ sec}^{-1}$ (solid circles). Same for $\bar{n} = 1$ (triangles). Rate expected for π^0 's vs. P_T (open circles).

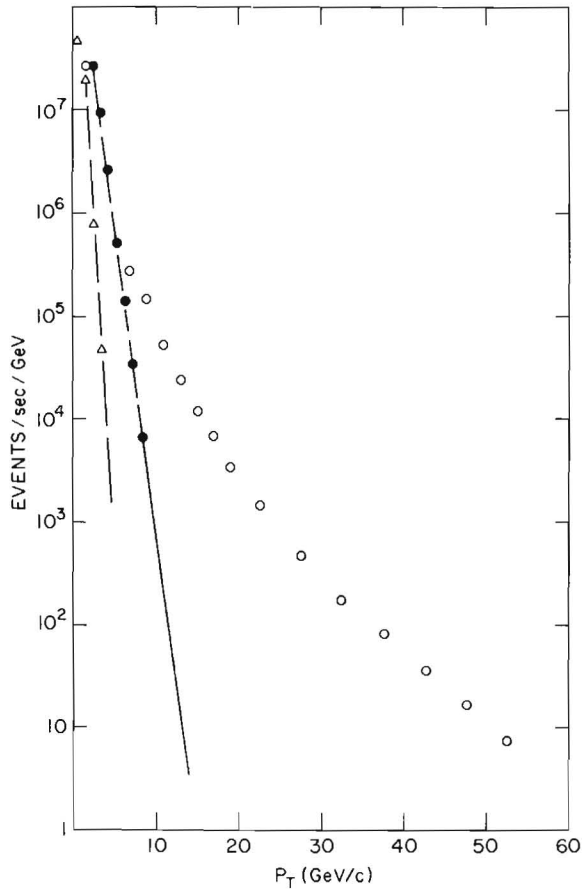


Figure 3. Rate of false triggers for the interval ($\Delta y = 1$, $\Delta\phi = \pi/2$) having the largest $\Sigma|P_T|$ from $\bar{n} = 10$ minimum bias events at $\sqrt{s} = 800$ GeV and $L = 10^{33} \text{ cm}^{-2} \text{ sec}^{-1}$ (solid circles). Only those towers with $P_T > 1$ GeV/c enter the sum. Same for $\bar{n} = 1$ (triangles). Rate expected from ISAJET for inclusive jet production vs. P_T (open circles).

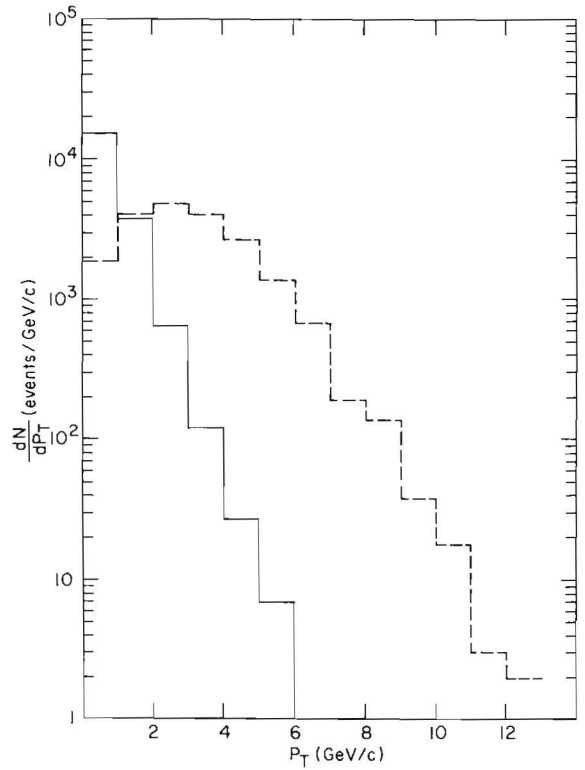


Figure 4. $\Sigma|P_T|$ for the fixed interval $-0.5 < y < 0.5$, $0 < \phi < \pi/2$. $\bar{n} = 10$ events (dashed line). Only those towers with $P_T > 1$ GeV/c enter the sum shown by solid line.